# Performance Measurements of a Unique Louver Particle Separator for Gas Turbine Engines

**Grant O. Musgrove**
Southwest Research Institute,
San Antonio, TX 78238
e-mail: grant.musgrove@swri.org

**Karen A. Thole**
Mechanical and Nuclear Engineering Department,
The Pennsylvania State University,
University Park, PA 16802

**Eric Grover**

**Joseph Barker**

United Technologies Corporation –
Pratt & Whitney,
East Hartford, CT 06108

*Solid particles, such as sand, ingested into gas turbine engines, reduce the coolant flow in the turbine by blocking cooling channels in the secondary flow path. One method to remove solid particles from the secondary flow path is to use an inertial particle separator because of its ability to incur minimal pressure losses in high flow rate applications. In this paper, an inertial separator is presented that is made up of an array of louvers followed by a static collector. The performance of two inertial separator configurations was measured in a unique test facility. Performance measurements included pressure loss and collection efficiency for a range of Reynolds numbers and sand sizes. To complement the measurements, both two-dimensional and three-dimensional computational results are presented for comparison. Computational predictions of pressure loss agreed with measurements at high Reynolds numbers, whereas predictions of sand collection efficiency for a sand size range 0–200μm agreed within 10% of experimental measurements over the range of Reynolds numbers. Collection efficiency values were measured to be as high as 35%, and pressure loss measurements were equivalent to less than 1% pressure loss in an engine application.* [DOI: 10.1115/1.4007568]

## Introduction

Aircraft gas turbines ingest solid particles during takeoff, landing, and while flying in dusty environments. The presence of solid particles in the engine flow path has been shown to reduce turbine power and efficiency [1]. Particle ingestion also reduces performance over the life of the engine through erosion, deposition, and blockage of cooling channels. Ingested particles pass through both primary and secondary flow paths in the turbine. In the primary flow path particles erode and deposit on airfoils resulting in rough airfoil surfaces that reduce engine efficiency and increase heat transfer to the airfoil. Deposition on turbine airfoils results in blocked film cooling holes and can cause engine surge when particulates build up on first stage turbine vanes [2,3]. Ingested particles that pass through the secondary flow path of the engine will reduce coolant flow by blocking cooling channels [4,5]. When coolant flow is reduced, the temperature of turbine components increases thereby reducing component life.

This paper presents performance measurements of a louver separator to remove solid particles, such as sand from the turbine secondary flow path. Performance measurements over a range of Reynolds numbers and sand sizes include pressure loss and particle collection efficiency. A unique method is developed to quantify particle collection efficiency in a laboratory setting. To compliment the data reported in this paper, two-dimensional and three-dimensional computational results are presented for direct comparison. This paper presents a review of relevant studies, methodology, measurement uncertainty and repeatability, and a discussion of results.

## Review of Relevant Literature

Methods to remove particles from gas turbine flows have included inertial particle separators because of their favorable characteristic to handle high flow rates at low pressure losses. Typically, inertial particle separators are placed at engine inlets exhausting the separated particles through a scavenge duct. The operating principle of inertial separators is to cause the particle-laden flow to abruptly change trajectory, whereby the particles do not react to the change in flow direction due to their larger inertia as compared to the flow. Such a separator is one that uses an array of louvers to change the flow direction.

The pressure loss and particle separation efficiency of louver separators are affected by Reynolds number, particle size, and louver geometry. Previous studies have reported that particle separation efficiency increased with inlet and scavenge Reynolds numbers [6–9]. Poulton and Cole [6] found that separation efficiency had an upper limit and leveled off at high inlet Reynolds numbers. Additionally, pressure losses resulting from the separator were reported by Smith and Goglia [7] and Poulton and Cole [6] to increase with Reynolds number. Besides increasing the inlet or scavenge Reynolds numbers, studies by Gee and Cole [8] and Poulton and Cole [6] showed that separation efficiency increased with particle size. However, particle mass loading (ratio of particle mass flow to air mass flow) was found to not affect separation efficiency [7,8].

The effect of the louver geometry on separation efficiency was studied with regard to louver angle, length, and spacing. Studies by Zverev [9] and Poulton and Cole [6] reported that particle separation efficiency was affected by louver angle by as much as 10%. Zverev [9] found that increasing the louver angle decreased the pressure loss of the separator. In contrast, louver length was shown by Gee and Cole [8] to increase separator pressure loss by as much as 40% when doubling the louver length. The spacing of the louvers in a separator array was reported by Zverev [9] and Poulton and Cole [6] to have low reduce separation efficiency when the spacing was small. Poulton and Cole [6] also showed that louver thickness affected the separation efficiency by no more than 10%.

Louver separator designs using scavenge flow are the most common geometries reported in the literature. A scavenge flow design, however, is not practical to remove solid particles from the secondary flow path within gas turbines because of flow path considerations. Others have investigated unique inertial separation methods that can be located within gas turbine flow paths.

Schneider et al. [10–13] did extensive experimental and computational investigations into the effectiveness of using a preswirl cavity to divert particles from internal cooling flow to the main flow path. More recent experimental work on using the preswirl

Contributed by the International Gas Turbine Institute (IGTI) of ASME for publication in the Journal of Engineering for Gas Turbines and Power. Manuscript received June 26, 2012; final manuscript received July 20, 2012; published online November 21, 2012. Editor: Dilip R. Ballal.

cavity to divert particles was completed by Villora et al. [14]. Syred et al. [15] computationally investigated a combustor design that integrated a particle removal system that removes both large and small particles. The can-type combustor removed large particles by acting as a cyclone separator. Small particles were separated by a vortex collector pocket located near the combustor exit. A louver separator using a static collection bin (collector) instead of a scavenge flow duct was studied by Musgrove et al. [16]. The louver separator trapped the separated particles in the collector and was intended for placement in the combustor-bypass flow. Musgrove et al. [16] computationally investigated the performance effects of area ratio (AR), louver geometry, and collector geometry. The bestdesign from the study consisted of an area ratio of 1.50 and eight straight louvers at varying angles ($\phi = 30$ deg to 45 deg to 30 deg), followed by a collector that produced a favorable circulation direction. Musgrove et al. [16] reported that the favorable circulation was necessary for particle collection by directing trapped particles away from the collector inlet. The presence of a vortex at the collector inlet (inlet vortex) was found to set up the favorable circulation in the collector.

This study presents measurements of two louver separator designs to complement the computational study presented by Musgrove et al. [16]. Both configurations have the same area ratio (AR = 1.50), number of louvers (eight), and identical collectors. The louver configurations include one that increments each louver angle along the array ($\phi = 30$ deg to 45 deg to 30 deg) while the second configuration maintains constant louver angle ($\phi = 45$ deg). Quantifying the separator performance consisted of measuring the pressure loss across the separator and the particle collection efficiency. Good performance of the separator was considered to be at low pressure loss with high particle collection efficiency. In addition to experimental measurements, results from both two- and three-dimensional computational models are compared.

## Experimental Facility and Methodology

The performance of a louver separator was evaluated from measured sand collection efficiency ($\eta$) and pressure loss coefficient ($C_p$). To evaluate the separator performance, an open loop test facility was constructed to make the measurements. The collection efficiency was calculated based on the mass of sand captured in the collector relative to the mass of sand subjected to the particle separator. The pressure loss coefficient was calculated from the static pressure loss across the separator relative to the dynamic pressure at the inlet to the test section enclosing the separator. In this section of the paper, the test facility, sand characterization, and louver separator configurations are explained in detail.

**Test Facility.** Testing was conducted in an open loop test facility that circulated in a clockwise direction, as indicated by the arrows in Fig. 1. Flow through the test facility was driven by a 0.66 $m^3/s$ (1400 CFM) blower powered by an 11 kW variable speed electric motor. Downstream of the blower, the flow passed through a pipe containing a venturi meter that was isolated upstream and downstream by 20 pipe diameters. Downstream of the venturi meter, the flow from the lower section of the test facility expanded through a transition into a rectangular channel. At the inlet to the rectangular channel, a honeycomb laminar flow element and splash plate were placed to produce spanwise uniform flow at the test section inlet. Additionally, the flow was tripped downstream of the channel inlet with sand paper placed along the top and bottom of the channel. Further downstream sand was injected across the span of the channel.

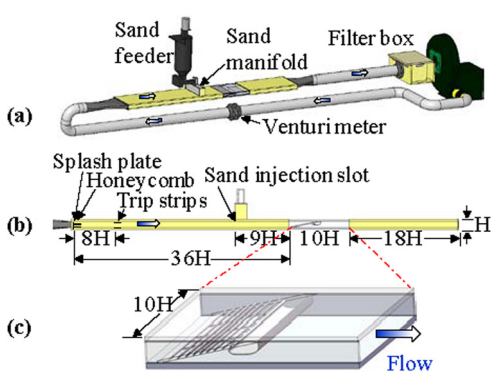


**Fig. 1 The (*a*),(*b*) open loop test facility included a sand injection system and (*c*) transparent test section**

The sand injection system was made up of a sand feeder, a mixing manifold, and an injection slot. The sand feeder, modified from commercial use as a plastics feeder, utilized a helical auger screw to convey sand from the feeder hopper into the mixing manifold at a constant flow rate. The flow rate was controlled by a variable speed motor coupled to the auger screw, where the maximum flow rate was determined by the size and number of threads of the auger screw. The maximum flow rate for the auger screw used in this study was 7 $cm^3/s$. In the mixing manifold, sand from the feeder was dispersed using compressed air injected through three ports. The objective of the compressed air was to both mix the sand and maintain slightly higher pressure in the manifold relative to the channel. The sand-air mixture in the manifold passed into the channel through a slot extending across the channel width. The slot was angled 45 deg upstream relative to the flow whereby the sand-air mixture was injected. Injecting the sand in the upstream direction ensured that sand particles were well mixed with the channel flow.

Downstream of the sand injection slot the louver separator was enclosed in a transparent test section, as shown in Fig. 1. The test section was constructed of transparent material to allow visual observation of sand trajectories through the louver array and in the collector. After passing through the separator, air flow and any uncollected sand passed through a downstream rectangular channel followed by a pipe and finally into a filter box. Any remaining sand in the flow was removed by three air filters placed in series in the filter box. As sand collected in the filters during each test, the increasing pressure loss across the filters reduced the test facility flow rate. The flow rate through the test facility, however, was decreased by no more than 2%.

As mentioned earlier, the pressure loss coefficient ($C_p$) was calculated from the dynamic pressure at the test section inlet, and the static pressure loss across the test section. The dynamic pressure was calculated based on the measured mass flow. Static pressures were measured at the inlet and exit of the test section. Spanwise uniformity of the flow through the louver separator was checked by normalizing the static pressure loss measurements. The pressure measurement at each tap was normalized from the difference of the tap pressure and the span wise average pressure divided by the inlet dynamic pressure. Flow uniformity was achieved when normalized values deviated by less than $\pm 5\%$.

After each test, the test facility was disassembled and all deposited sand mass was carefully removed and weighed. To give an accurate account of the collection efficiency ($\eta$), a methodology was developed that allowed a true accounting of all of the sand placed in the feeder. This accounting was needed to include any sand that remained in the feeder, deposited on the channel walls, and was collected in the downstream filters. For most tests, between 90–95% of the injected sand was accounted for, as will be shown in the results. To calculate the collection efficiency, the sand trapped in the collector ($m_{col}$) was divided by the sand that passed through the test section inlet ($m_{in}$). The sand that was considered to be collected was that amount accumulated in the collector. The sand that passed through the test section inlet was considered to be the sand placed in the feeder prior to a test minus the sand that remained upstream of the test section after a test. The amount of sand upstream of the test section after a test was

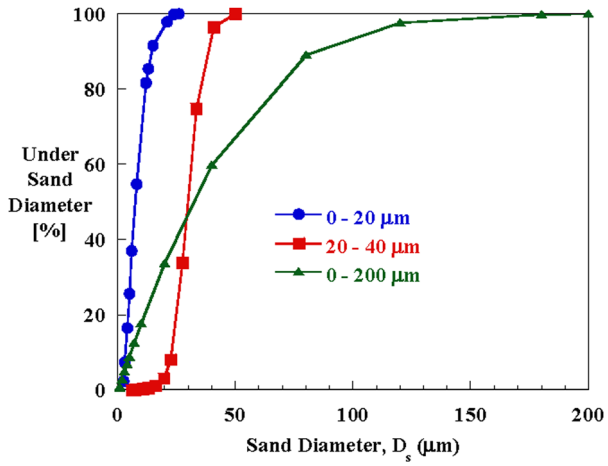


**Fig. 2 Particle size distribution by percent volume of ISO 12103-1 A4 test sand [17]**

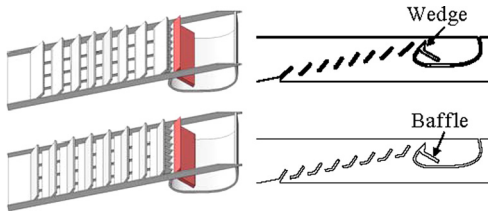


**Fig. 3 The (upper) variable and (lower) constant louver configurations included structural supports and a wedge and baffle at the collector inlet**

**Table 1 Area ratio and louver geometry**

| | Variable louver | Constant louver |
|---|---|---|
| Area ratio (AR) | 1.50 | 1.50 |
| Number of louvers | 8 | 8 |
| Louver angle ($\phi$) | 30 deg to 45 deg to 30 deg | 45 deg |

found deposited in the feeder ($m_{feed}$), on the upstream walls ($m_{chan}$), and was left in the mixing manifold ($m_{man}$). Sand also deposited on the louver surfaces during testing; however, this amount was usually negligible. The sand that collected in the filters was considered to be the amount that was not successfully collected by the louver separator. The filters were weighed before and after each test to determine the amount of sand that the collector did not capture. The largest amount of sand recovered from the test facility was in the filters and the sand feeder. After the deposited sand was removed, all surfaces were wiped clean to remove sand residue. It is important to point out that prior to each test; the injected sand was heated at 100 °C for at least three hours to remove any moisture.

**Sand Characterization.** The coarse sand used in this study was ISO 12103-1 A4 certified sand with a bulk density of 1201 kg/m$^3$, purchased from Powder Technology Inc. Five size ranges of the test sand were studied to determine the effect of sand size on collection efficiency: 0–200 $\mu$m (entire sample size), 0–20 $\mu$m, 20–40 $\mu$m, 38–63 $\mu$m, and 63–200 $\mu$m. Size ranges purchased from Powder Technology Inc. included 0–200 $\mu$m, 0–20 $\mu$m, and 20–40 $\mu$m with size distributions shown in Fig. 2 [17]. Sand size ranges of 38–63 $\mu$m and 63–200 $\mu$m were obtained by filtering the 0–200 $\mu$m size distribution through sieves. The size ranges of the sieved sand were obtained by sieving the sand through mesh screens with screen opening sizes corresponding to the maximum or minimum desired sand size. For example, the 63–200 $\mu$m size range was obtained by filtering the 0–200 $\mu$m range through a sieve with mesh screen opening sizes of 63 $\mu$m.

**Louver Separator Geometry.** The two louver separators studied in this paper were similar to configurations presented in a previous computational study [16]. Each louver separator was made up of an array of straight louvers followed by a collector. One configuration had a varying louver angle and the second configuration had a constant louver angle, as shown in Fig. 3. In the previous study, the louver angles were varied with different distributions to try to improve collection efficiency. The variable louver angle configuration used in this study was found previously (Musgrove et al. [16]) to have the highest particle collection efficiency of all the configurations that were simulated. A primary flow feature of the variable angle configuration that was found necessary for high collection of small particles is the setup of a vortex at the inlet to the collector. Constant angle configurations were not found to setup the inlet vortex, for the current collector design, and consequently had collection efficiencies less than the variable louver configuration. In contrast to the variable louver configuration, a constant louver angle design is also tested in this study to represent a baseline case from the previous study. Details of each configuration are listed in Table 1.

The most noticeable differences between the cross sections of the two designs are the orientation angles of the louvers and the length of the louver anchors. The louver anchors are defined as the short length of each louver that lies along the axis of the louver array. The differences in louver anchor lengths between the two configurations are primarily dependent on the louver orientation angles ($\phi$), as shown in Fig. 4. From the orientation angle, the louver lengths (L) are determined for a prescribed area ratio (AR) such that the anchor length is equal to the diagonal distance between louvers minus the louver length. Therefore, an increasing louver orientation angle results in a decreasing louver length and an increasing louver anchor length. For example, the louver lengths of the constant louver angle configuration are shorter than the variable louver configuration because most of the louver angles are larger. Furthermore, it should be expected that in the variable louver angle configuration the louver anchor immediately downstream of the 45 deg louver should have a length comparable to the constant louver configuration. However, the louver anchor lengths of the variable louver configuration were modified from the previous computational study [16] to include part thickness and still maintain the design area ratio (AR) of 1.50. Modifications included the adjustment of louver spacing, louver anchor length, and the axial position of the collector inlet. The modifications were determined to not affect the overall performance of the separator by comparing two-dimensional computational results of the modified configuration in this study to the configuration in the

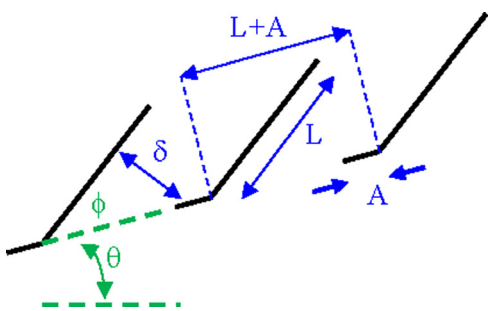


**Fig. 4 The louver anchor length (A) is determined by subtracting the louver length (L) from the distance between louvers (L+A)**

**Table 2 Effect of collector modifications**

| | | |
|---|---|---|
| No modification | 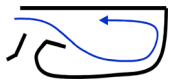 | $\eta = 0\%$ |
| Baffle | 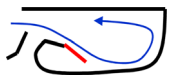 | $\eta = 3\%$ |
| Wedge | 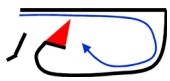 | $\eta = 0\%$ |
| Wedge and baffle | 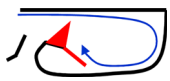 | $\eta = 20\%$ |

previous study [16]. In addition, a total of 10 structural supports were added at spanwise intervals to the design to resist the flow drag force and maintain correct louver spacing and angle. Three louver supports were placed under the louver array, and seven supports were placed between the last louver and the collector.

The design specified in the previous computational study [16] was tested to find negligible sand collection due to the observed collector circulation that directed sand towards the collector inlet (unfavorable circulation). The observed circulation opposite to the favorable circulation predicted in the previous computational study [16]. Therefore, the collector inlet was modified to improve sand collection efficiency. Modifications that were made to the collector inlet were guided by the experimentally observed sand circulation in the collector. Table 2 illustrates different collector inlet geometries that were tested, and their resulting collection efficiency. A baffle, shown in Table 2, slightly improved collection efficiency by isolating the region of the collector under the baffle from the unfavorable circulation. A second modification placed a wedge at the collector inlet to converge the collector inlet flow against the top wall of the test section. The wedge produced a favorable circulation in the collector that directed sand away from the collector inlet; however, sand that entered the collector was not trapped. Use of the wedge or baffle modifications independently did not significantly improve collection efficiency. Collection efficiency was improved, however, when the wedge and baffle were used together. The favorable circulation set up by the wedge directed sand away from the collector inlet and into the isolated region created by the baffle. Furthermore, there was no notable increase in pressure loss as a result of the wedge and baffle.

Results reported in this paper are for both of the louver configurations shown in Fig. 3 with the inclusion of the wedge and baffle modification. The performance of each separator configuration is expressed in terms of collection efficiency ($\eta$) and pressure loss coefficient ($C_p$).

## Computational Methodology

In addition to experimental measurements, two-dimensional and three-dimensional computational models were simulated over the same range of Reynolds numbers and sand sizes in the experiment. The computational study was motivated by the difference between the measurements and two-dimensional predictions [16] of collection efficiencies of both separator configurations without the wedge and baffle modification. All computational models were solved using FLUENT 6.3.26 [18], similar to the methodology followed by Musgrove et al. [16] in solving the flow field and particle trajectories.

Each simulation was matched to the experimental flow conditions and geometry including the wedge and baffle modification. The length of the computational domain matched the experiment from the sand injection slot to the exit of the downstream channel. Both two-dimensional and three-dimensional models used boundary conditions of inlet velocity and exit outflow with no-slip surfaces for all remaining surfaces. The three-dimensional model used a symmetry boundary condition at a spanwise depth of 5 H. Two-dimensional and three-dimensional grid sizes of $6 \times 10^4$ and $3 \times 10^6$ cells were required for second order accurate grid independent solutions that met a convergence criterion of $10^{-6}$. Solutions used steady RANS equations and the k-$\omega$ turbulence model. Both computational models utilized a boundary layer mesh along the top and bottom walls of the test section with $y^+ = 30$.

Pressure loss coefficients ($C_p$) were calculated from integrating mass averaged total pressure and area averaged dynamic pressure at locations consistent with the inlet and exit static pressure taps in the test facility. Similar to Musgrove et al. [16], the collection efficiency was calculated from the number of sand particles injected into the domain relative to those that escaped the domain. Sand was injected along the channel height at an upstream location consistent with the injection slot in the test facility. Sand sizes 1–200 $\mu$m with bulk density 1201 kg/m$^3$ were injected whereby the particle trajectories were simulated using FLUENT's discrete phase model with particle restitution coefficient of 1.0 and shape factor of 1.0. To obtain collection efficiency values independent of the number of particles injected, 1000 particles were injected across the channel height. For the three-dimensional simulation, 1000 particles were injected at spanwise intervals of 0.125 H for each sand size. Because the computational predictions used numbers of sand particles instead of sand mass to calculate collection efficiency, the computational results were converted to a mass weighted equivalent. A mass weighted value that could be directly compared to experimental data was obtained by integrating the predicted collection efficiency values with respect to sand size and normalizing by the integrated size range.

## Measurement Uncertainty and Repeatability

The uncertainty analysis for collection efficiency and pressure loss coefficient followed the partial derivative method described by Moffat [19]. Overall uncertainty was calculated from the root sum square of the precision and bias errors. The precision error was calculated from the standard deviation of five sets of measurements, where each set consisted of three tests. Each test measured pressure loss coefficient and collection efficiency for similar Reynolds number, sand amount, and mass loading.

Precision uncertainty values of $\pm 0.078$ for $C_p$ and $\pm 0.026$ for $\eta$ were calculated using a 95% confidence interval on Student's t-distribution. The calculated bias error due to the measurement devices had maximum values of $\pm 2.14$ for $C_p$ and $\pm 0.02$ for $\eta$. The bias and precision errors were combined to determine the overall uncertainty of each calculation. The constant louver configuration had an overall uncertainty of $\pm 11\%$ for $C_p = 20.0$ and $\pm 3\%$ for $\eta = 35\%$ at $Re = 8000$. Overall uncertainty for the same configuration at $Re = 46{,}400$ was $\pm 3\%$ for $Cp = 12.1$ and $\pm 3\%$ for $\eta = 8\%$. Because the overall uncertainty values obtained in this manner were acceptable values, the measurements reported in this paper were an average of three tests.

Experimental repeatability was confirmed for each test by recording the amount and location of sand deposited in the test facility. The mass of deposited sand was dependent on the amount of sand placed into the feeder ($m_0$) and the sand mass loading (ML). Therefore, $m_0$ and ML were varied to determine the effect on collection efficiency, and to verify the repeatability of the sand retrieval method. Sand amounts of 60 g, 180 g, and 240 g were tested at constant ML = 0.002. Mass loading values of 0.0002, 0.002, and 0.02 were tested for constant $m_0 = 60$ g. Mass loading was limited to values much less than one so that particle-particle interactions and particle effects on the flow field could be ignored [20], which is representative of engine ingestion. Reynolds number ($Re = 25{,}000$), sand size distribution ($0 < D_s < 200\ \mu$m), and separator configuration (variable louver) were held constant for each sand amount and mass loading test. Varying the mass

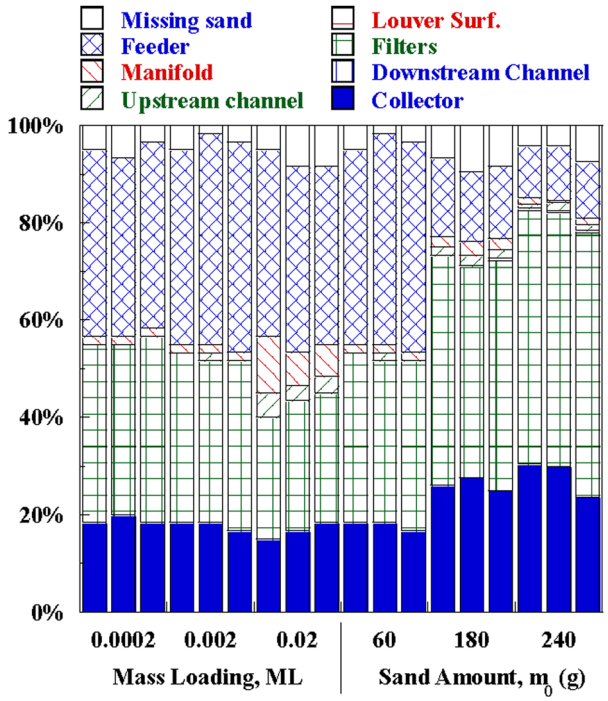


**Fig. 5 Test repeatability was indicated by the similar sand deposition in the test facility for varying ML and $m_0$ for the variable louver configuration at Re = 25,000 for $0 < D_s < 200\ \mu m$**

loading and sand amount did not affect the collection efficiency of the variable louver separator.

The repeatability of each sand test was confirmed by comparing the deposited sand amounts among each set of three tests, as shown in Fig. 5. Sand that was removed upstream of the test section included sand that remained in the feeder and sand adhering to the manifold and upstream channel walls. Deposited sand in the test section was adhered to the louvers and trapped in the collector. Downstream of the test section sand adhered to the downstream channel walls and collected in the filters. Sand deposition in the test facility is shown in Fig. 5 as percentage of sand amount ($m_0$) for varying ML and $m_0$. The similar amounts of sand retrieved from the sections of the test facility for each set of tests indicated repeatable sand flow. For all tests, the missing sand amount was consistently less than 10% of the initial sand amount ($m_0$). Sand deposition in the manifold and upstream channel was higher for ML = 0.02 than lower mass loadings because the flow rate of the compressed air injected into the manifold was not enough to disperse the high flow rate of sand from the feeder. The high amount of deposited sand in the manifold and upstream channel reduced the amount of sand that was collected by the filters, but did not affect the amount of sand captured in the collector. The percentage of sand in the filter and collector, however, increased with $m_0$ because more sand passed through the test facility with an unchanged amount of sand remaining in the feeder.

Figure 6 shows that collection efficiency was independent of sand amount and mass loading for sand sizes 0–200 $\mu$m. Changing the mass loading and sand amount was shown in Fig. 5 to affect deposited sand amounts throughout the test facility. Therefore, collection efficiency was independent of sand deposition in the test facility. The variable louver configuration resulted in measured collection efficiency of $\eta = 32\%$ at Re = 25,000 for all tested values of $m_0$ and ML. Repeatable tests of varying mass loading (ML) and sand amount ($m_0$) did not affect sand collection efficiency of sand sizes 0–200 $\mu$m for the variable louver separator at Re = 25,000. Therefore, all tests used sand amount and mass loading values of $m_0 = 60$ g and ML = 0.002.

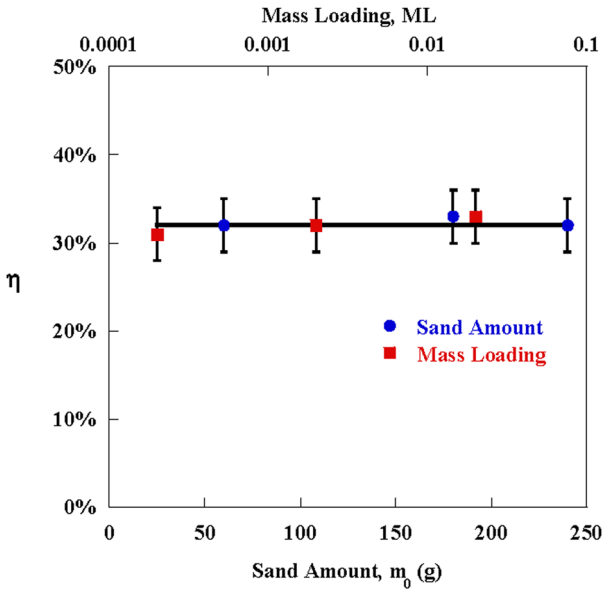


**Fig. 6 Collection efficiency was independent of ML and $m_0$ for the variable louver configuration at Re = 25,000 for $0 < D_s < 200\ \mu m$**

## Discussion of Results

As was stated, each louver separator was tested over a range of Reynolds numbers and sand sizes at a constant mass loading (ML = 0.002) and sand amount ($m_0 = 60$ g). Tests over the range of Reynolds numbers injected the sand size distribution with size range 0–200 $\mu$m. Effects of sand diameter were tested at constant Reynolds number (Re = 46,400) by injecting discrete size intervals. In addition to pressure loss and collection efficiency results, sand distribution through the test facility and images of sand accumulation in the collector are presented. Results from both the two-dimensional and three-dimensional models are presented along with measurements for direct comparison.

**Pressure Loss Results.** Measured and predicted pressure loss coefficients ($C_p$) for both separator configurations are shown in Fig. 7 for a range of Reynolds numbers. The similar $C_p$ values for both configurations indicated that louver angle did not significantly affect pressure loss. These measured pressure loss coefficients translate to losses that can occur in the engine. The

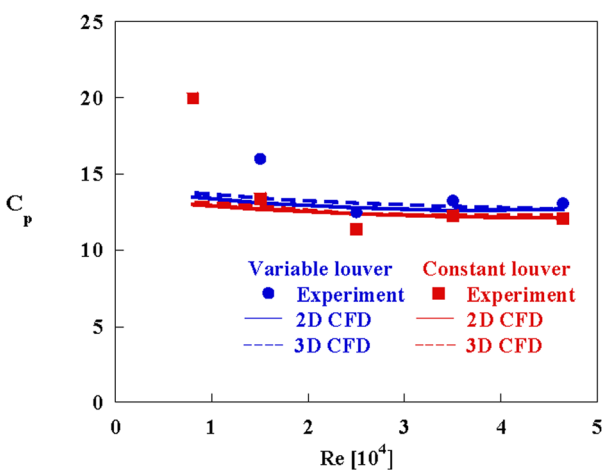


**Fig. 7 Pressure loss across both separator configurations increased for decreasing Reynolds numbers**

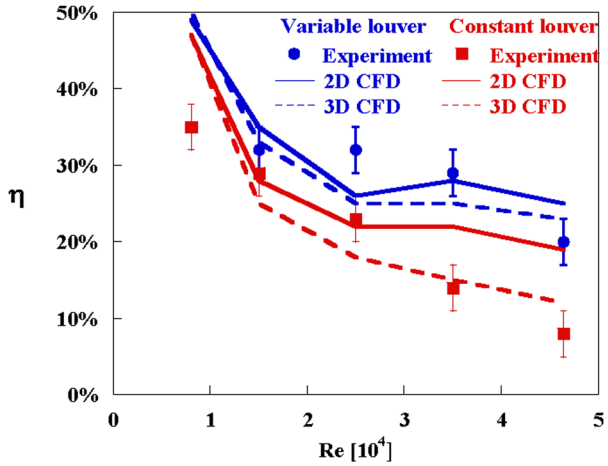


**Fig. 8 The collection efficiency for both configurations increased as Reynolds number decreased for $0 < D_s < 200\ \mu m$**

maximum measured pressure loss coefficient for the constant louver configuration ($C_p = 20$) is equivalent to a 0.7% pressure loss in the engine. The minimum measured pressure loss coefficient ($C_p = 12.1$) is equivalent to a 0.4% loss.

Computational predictions of $C_p$ agreed with data for Reynolds numbers greater than 25,000; however, pressure loss coefficients were under-predicted at lower Reynolds numbers. The disagreement between measurements and predictions at low Reynolds numbers was most likely because the predictions did not show that the flow around the louvers changed with Reynolds number. Computational simulations predicted similar separation regions on the backside of the louvers for all Reynolds numbers. It was expected, however, that the measured pressure loss increased for low Reynolds numbers because the size of the separation regions increased. Furthermore, little difference was seen between the two-dimensional and three-dimensional pressure loss predictions because spanwise flow effects were not apparent.

**Reynolds Number Effects on Collection Efficiency.** Contrary to similar pressure losses between both louver configurations, collection efficiency was significantly affected by the two different louver arrays. The results reported in Fig. 8 include experimental and computational results for injecting the 0–200 $\mu$m sand for varying Reynolds numbers.

The variable louver configuration results in Fig. 8 were found experimentally and computationally to collect more sand than the constant louver configuration at all Reynolds numbers. As Reynolds number decreased, the two louver configurations approached similar collection efficiencies. At low Reynolds numbers, the variable louver configuration had a maximum collection efficiency of 32%. The constant louver configuration had increasing collection efficiency with decreasing Reynolds number to a maximum measured value of 35% at $Re = 8000$. Reynolds numbers less than 8000 were not tested because the channel flow velocity was not sufficient to carry the sand particles downstream. Collection efficiency of both separator configurations was measured to increase for decreasing Reynolds numbers because the momentum of the sand particles decreased with decreasing Reynolds number. As the momentum of the sand particles was reduced, the particles were more susceptible to fall out of the collector circulation and remain in the collector, which will be explained in more detail later. It is interesting to note that the trend of collection efficiency over the Reynolds number range found for the louver configurations differ from separator designs with scavenge ducts.

To compliment the measured collection efficiency, photographs were taken of sand accumulation in the collector for each Reynolds number tested. Sand collection was observed to be repeatable

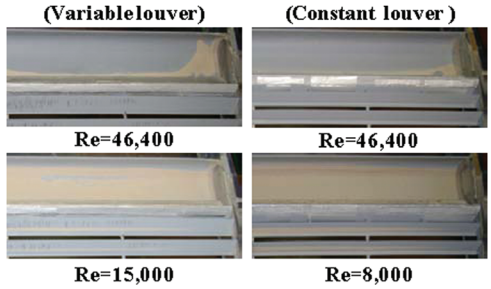


**Fig. 9 Sand was uniformly collected across the collector span in increasing amounts with decreasing Reynolds number for $0 < D_s < 200\ \mu m$**

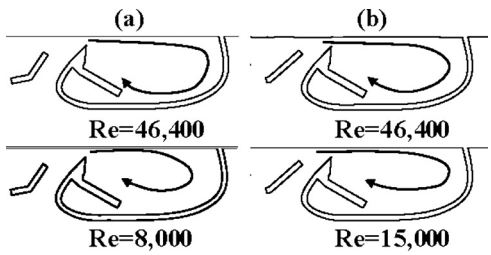


**Fig. 10 Circulation size was observed to decrease with decreasing Reynolds number for the (*a*) constant and (*b*) variable louver configurations for $0 < D_s < 200\ \mu m$**

and uniformly symmetric about the midspan of the test section. Figure 9 shows half span images of sand accumulation at the minimum and maximum Reynolds numbers for both louver designs. Comparison of the images confirmed more sand was collected at lower, rather than higher, Reynolds numbers. For low Reynolds numbers, sand accumulation was concentrated on the bottom wall of the collector out-from-under the baffle. For higher Reynolds numbers, sand accumulated under the baffle and at the ends of the collector. The change in accumulation location is explained by visual observations of sand trajectories in the collector. The circulation size in the collector was observed to increase with Reynolds number, as shown in Fig. 10. The large circulation directed particles under the baffle resulting in more sand accumulation under the baffle at high Reynolds numbers. The small circulation at low Reynolds numbers resulted in sand depositing in the collector out-from-under the baffle.

To confirm the repeatability of each sand test the deposited sand mass throughout the test facility was removed and measured, as shown in Figs. 11 and 12 as a percentage of the total sand injected. Most of the sand retrieved from the test facility was located in the filters and the feeder. The percentage of sand depositing upstream of the test section remained constant over the range of Reynolds numbers for both louver configurations. The percentage of sand depositing in the filters was dependent on the amount of sand captured by the collector. The similar sand deposition between the tests for each Reynolds number indicated repeatable sand flow through the test facility. For most tests, more than 90% of the injected sand amount was retrieved.

As shown in Fig. 8, both two-dimensional and three-dimensional computational models predicted values of collection efficiency within 10% of measured data. The predicted trends, however, disagreed with the experimental trends. The two-dimensional computational models predicted that both louver configurations had the same trend in collection efficiency. In comparison, measurements indicated that the trend was affected by the louver configuration. Measurements of collection efficiency showed that the variable louver configuration leveled off at low Reynolds numbers and the constant louver configuration

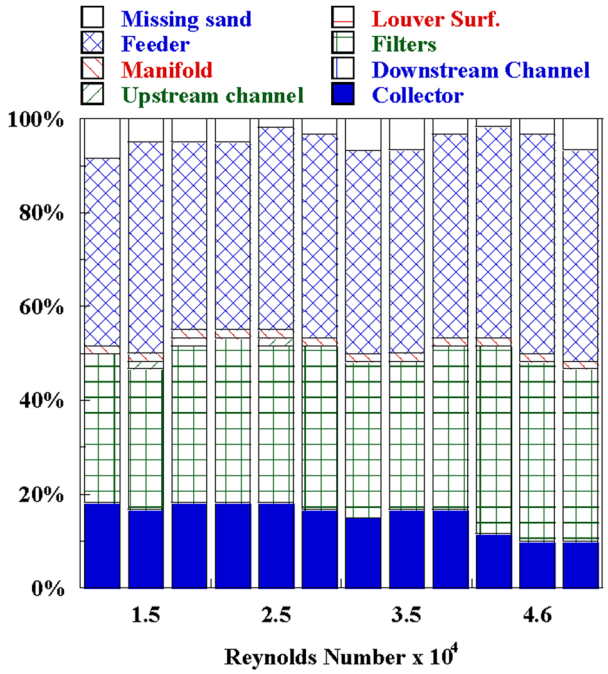


**Fig. 11 Distribution of sand through the test facility for the variable louver configuration when varying Reynolds number for 0 < Ds < 200 $\mu$m**

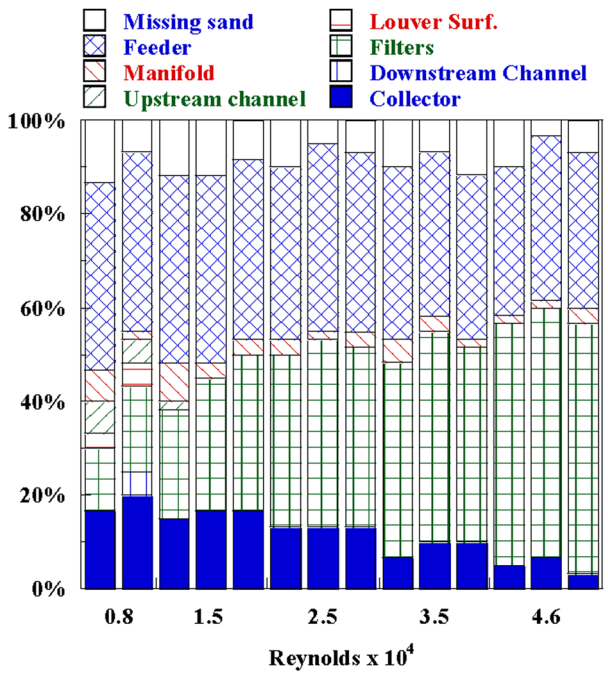


**Fig. 12 Distribution of sand through the test facility for the constant louver configuration when varying Reynolds number for 0 < $D_s$ < 200 $\mu$m**

continued to increase for low Reynolds numbers. Computational models predicted that the collection efficiency of both louver configurations increased for decreasing Reynolds numbers.

It is also of importance that the two-dimensional and three-dimensional predictions for the variable louver configuration were nearly the same, whereas the two-dimensional and three-dimensional predictions for the constant louver configuration were different. The reason the two-dimensional model for the constant louver configuration predicted higher collection efficiency than the three-dimensional model resulted from spanwise flow effects in the three-dimensional predictions. The spanwise flow was observed from the three-dimensional model results to be caused by the test section endwalls and disrupt the favorable collector circulation, thereby reducing the effectiveness of the collector. The favorable circulation was disrupted for the constant louver configuration and not the variable louver configuration because the constant louver configuration had a weaker collector circulation than the variable louver configuration. The presence of the favorable circulation has been shown in a previous computational study to occur with an inlet vortex [16]. The strength of the collector circulation and inlet vortex was shown to significantly affect the collection efficiency and to be dependent on the louver configuration [16]. Computational predictions of both louver configurations converged for low Reynolds numbers because at low Reynolds numbers the effect of the louver configuration on the inlet vortex was reduced.

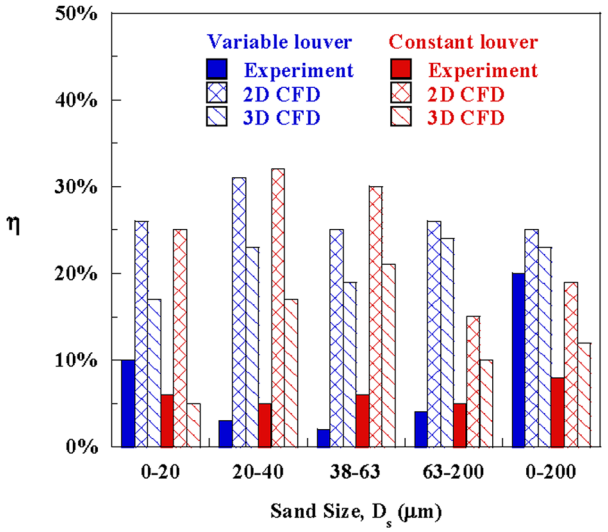


**Fig. 13 Collection efficiency was dependent on sand size and louver configuration at Re = 46,400**

**Sand Size Effects on Collection Efficiency.** In addition to Reynolds number effects, the influence of sand size on the collection efficiency was also tested. Four discrete sand size intervals were independently injected, sizes: 0–20 $\mu$m, 20–40 $\mu$m, 38–63 $\mu$m, and 63–200 $\mu$m. For each sand size interval the Reynolds number, mass loading, and injected sand amount were held constant (Re = 46,400, ML = 0.002, $m_0$ = 60 g).

Measured results indicated that the effect of sand size on collection efficiency was dependent on the louver configuration, as shown in Fig. 13. Specifically, the collection efficiency of the variable louver configuration was dependent on sand size, while the constant louver configuration was not. The variable louver configuration was best at collecting sand sizes less than 20 $\mu$m in diameter with reduced collection efficiencies for sizes larger than 20 $\mu$m. Injecting the entire sand size distribution (0–200 $\mu$m) resulted in as much as 20% higher collection efficiency for the variable louver collection efficiency compared to injecting only discrete sand sizes. The collection efficiency of the constant louver configuration, however, was independent of the injected sand sizes. Injecting the entire sand size range (0–200 $\mu$m) resulted in similar collection efficiency as injecting any of the discrete sand size intervals. Furthermore, it was likely that small particles agglomerated to create large particles in the collector because combining the collection efficiency for each discrete sand size was not equivalent to the collection efficiency of injecting all sizes together (0–200 $\mu$m).

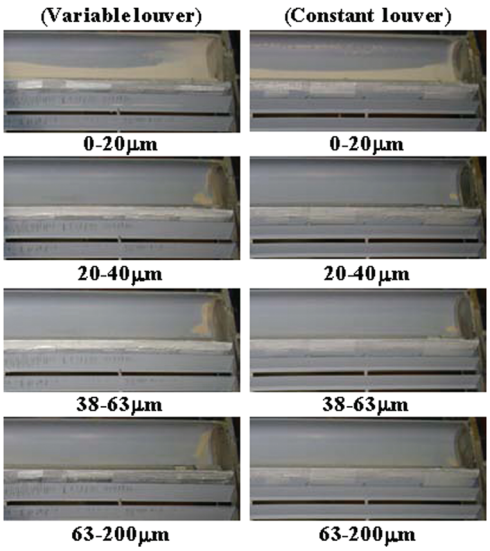


**Fig. 14 Sand sizes $D_s < 20\,\mu m$ were distributed evenly across the collector; however, sizes $D_s > 20\,\mu m$ deposited only at the collector ends for Re = 46,400**

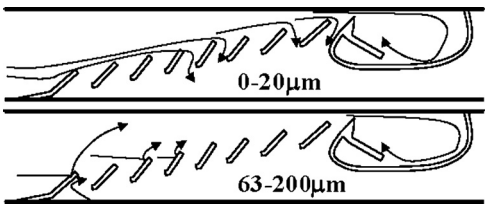


**Fig. 15 Large sand sizes were observed to not follow streamlines through the variable louver configuration at Re = 46,400**


**Fig. 16 Large sand sizes were observed to not follow streamlines through the constant louver configuration at Re = 46,400**

The accumulation pattern of sand in the collector was observed to be dependent on particle size. Accumulation in the collector was repeatable and symmetric about midspan with the half span shown in Fig. 14. Accumulation patterns were similar for both louver configurations for varying sand sizes. Sand sizes less than 20 $\mu$m in diameter were evenly distributed across the span of the collector for both separator configurations where most accumulation occurred on the bottom of the collector out-from-under the baffle. Sizes larger than 20 $\mu$m accumulated in small amounts near the ends of the collector. The increased sand accumulation for small sand sizes can be explained with observations of sand trajectories through the separator. Sand trajectories are shown in Figs. 15 and 16 for minimum and maximum sand size intervals. For small sand sizes, sand trajectories appeared to follow flow streamlines. Increasing the sand size resulted in increased deflections from the louver and test section surfaces. In the collector, the circulation size and rotation of sand entrained in the flow appeared to be independent of sand size. The mechanism responsible for sand trajectories in the collector was probably different

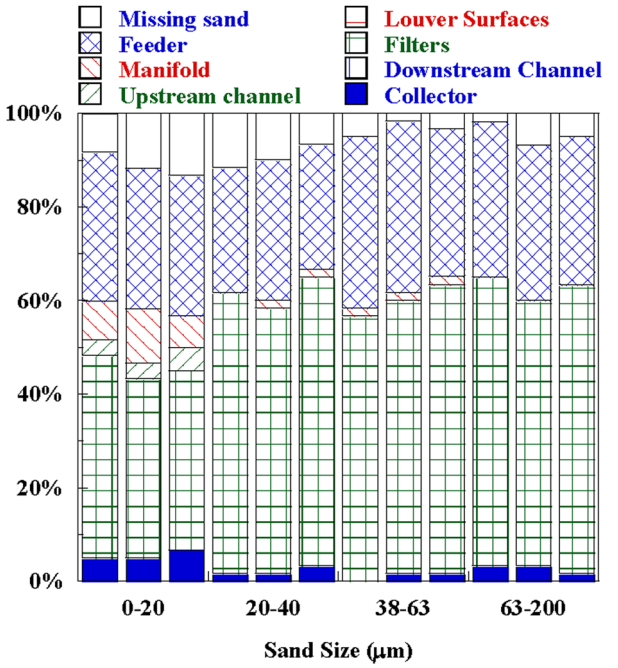


**Fig. 17 Distribution of sand through the test facility for variable louver angle when varying sand size at Re = 46,400**

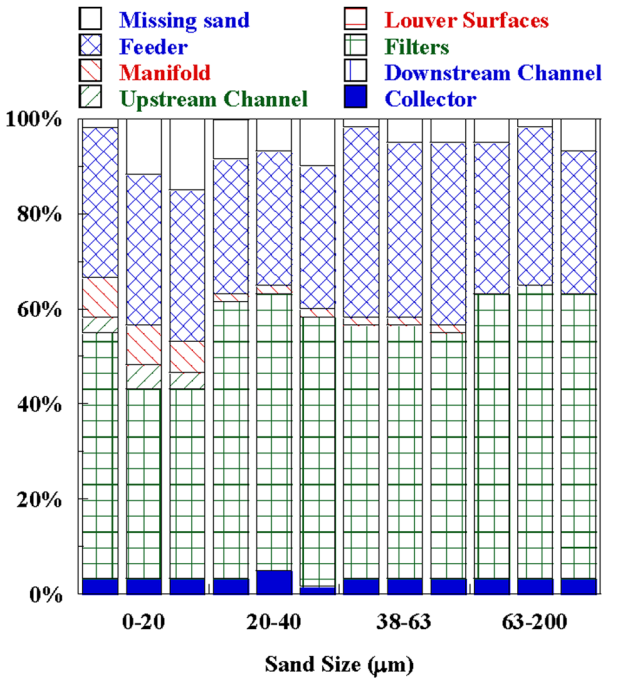


**Fig. 18 Distribution of sand through the test facility for constant louver angle when varying sand size at Re = 46,400**

for large sand sizes relative to small sand sizes. Large sand sizes were likely conveyed by their deflection from the collector walls while small sizes were likely convected by flow circulation in the collector.

To confirm test repeatability, the distribution of deposited sand throughout the test facility was recorded for the different sand size intervals that were injected. The deposited sand amounts that were retrieved after each test are shown in Figs. 17 and 18 as a percentage of injected sand amount ($m_0$). For the small size range (0–20 $\mu$m), most of the deposited sand was due to adherence to

the test facility walls. In contrast, large sand sizes did not deposit upstream of the test section, and were more easily caught in the filters than the small sand sizes. Therefore, tests with large sand sizes resulted in less sand amount missing.

Comparison of measurements to computational results showed that computational models over-predicted collection efficiency for all size intervals, as shown earlier in Fig. 13. The over-prediction indicated that the models did not completely agree with the measured data; however, the three-dimensional predictions were lower than two-dimensional predictions. The trend in predicted collection efficiency can be explained by considering the two-dimensional predictions. The two-dimensional predictions indicated an increase followed by a decrease in collection efficiency with increasing sand size. This change in efficiency was caused by the differences between the particle momentum (increasing with sand size) and flow field velocities. Increasing the size range from 0–20 $\mu$m to 20–40 $\mu$m increased particle momentum such that particles were separated by the louver array and passed into the collector where they were captured. Further increasing sand size imparted too much momentum such that deflections through the louver array caused the particles to either not be separated by the louver array, or to deflect from the collector walls and escape. The three-dimensional trend followed the increasing and decreasing two-dimensional trend of collection efficiency for similar reasons. The spanwise flow in the collector, however, complicated sand trajectories that resulted in the three-dimensional trend deviating from the two-dimensional trend for some sand size intervals.

## Conclusions

This paper has presented pressure loss and collection efficiency measurements for two louver separator configurations. One separator had a varied louver angle along the array ($\phi = 30$ deg to 45 deg to 30 deg), and the second separator had constant louver angle along the array ($\phi = 45$ deg). Both configurations were tested in a unique test facility over a range of Reynolds numbers and sand sizes. Both two-dimensional and three-dimensional computational predictions were presented along with measurements.

The pressure loss coefficients of both separator configurations were shown to increase for decreasing Reynolds numbers. The similar pressure loss coefficients between the two louver configurations indicated that louver angle did not significantly affect separator pressure loss. The louver angle, however, did significantly affect the collection efficiency of the separator over the range of Reynolds numbers. The collection efficiency of both the variable and constant louver configurations increased to similar values for decreasing Reynolds numbers. The variable louver configuration leveled off at $\eta = 32\%$ for low Reynolds numbers, and the constant louver configuration continued to increase to a maximum measured collection efficiency of 35% at Re = 8000.

The sand circulation pattern in the collector was observed to increase in size with Reynolds number. The change in circulation size affected sand accumulation in the collector. Sand accumulated under the baffle in the collector at high Reynolds numbers because the large circulation size directed particles under the baffle. At low Reynolds numbers, however, the small circulation size caused sand to accumulate on the bottom of the collector out-from-under the baffle.

The effect of sand size on collection efficiency was investigated by injecting discrete size intervals. The collection efficiency of the variable louver configuration was affected by sand size; however, the collection efficiency of the constant louver configuration was independent of sand size. The variable louver configuration was found to best collect sand sizes less than 20 $\mu$m compared to collecting larger particles. Sand collection was best, however, when the entire size range (0–200 $\mu$m) was injected. The collection efficiency was unchanged, however, for the constant louver configuration for any sand size interval.

Both two-dimensional and three-dimensional computational models were used to predict collection efficiency and pressure loss. For varying Reynolds numbers computational predictions were within 10% of measured collection efficiency values, and agreed with pressure loss coefficient data at high Reynolds numbers. The predicted trends, however, did not agree with measurements over the range of Reynolds numbers. The collection efficiency trend for increasing sand size did not agree with measurements. Collection efficiency was over-predicted for all discrete sand size intervals.

In conclusion, this paper has presented results that indicate particle collection efficiencies greater than 30% can be obtained for an inertial louver separator that uses a static collector. Two-dimensional and three-dimensional computational predictions were in agreement with some measured values; however, computational predictions did not match measured collection efficiency trends.

## Acknowledgment

The authors would like to thank Pratt & Whitney for funding and sponsoring this research effort, including Joel Wagner, Ryan Levy, and Takao Fukuda.

## Nomenclature

- A = louver anchor length
- AR = area ratio AR = $\delta$(# Louvers)/H
- $C_p$ = pressure loss coefficient $C_p = (P_{inlet} - P_{exit})_{static}/(P_{inlet})_{dyn}$
- $D_s$ = sand particle diameter
- H = height of test section and test facility channel
- L = louver length, L = (AR*H)/(# louvers*sin$\theta$)
- m = mass of sand
- ML = mass loading, ML = (sand mass flow rate)/(fluid mass flow rate)
- Re = test section inlet Reynolds number $Re = \rho H U_{in}/\mu$
- $U_{in}$ = test section inlet flow velocity

## Greek

- $\delta$ = louver gap
- $\eta$ = collection efficiency, $\eta = m_{col}/m_{in}$
- $\mu$ = fluid dynamic viscosity
- $\rho$ = fluid density
- $\phi$ = louver orientation angle
- $\theta$ = angle between the louver array axis and the horizontal

## Subscripts

- 0 = sand initially placed in sand feeder
- col = sand collected in the collector after a test
- chan = sand deposited in the upstream channel
- feed = sand remaining in the feeder
- in = sand entering the test section, $m_{in} = m_0 - m_{feed} - m_{man} - m_{chan}$
- man = sand deposited in the mixing manifold

## References

[1] Tabakoff, W., Hosny, W., and Hamed, A., 1976, "Effect of Solid Particles on Turbine Performance," ASME J. Eng. Power, **98**(1), pp. 47–52.
[2] Kim, J., Dunn, M. G., Baran, A. J., Wade, D. P., and Tremba, E. L., 1993, "Deposition of Volcanic Materials in the Hot Sections of Two Gas Turbine Engines," ASME J. Eng. Gas Turbines Power, **115**, pp. 641–651.
[3] Dunn, M. G., Baran, A. J., and Miatah, J., 1994, "Operation of Gas Turbine Engines in Volcanic Ash Clouds," ASME Paper No. 94-GT-170.
[4] Walsh, W. S., Thole, K. A., and Joe, C., 2006, "Effects of Sand Ingestion on the Blockage of Film-Cooling Holes," ASME Paper No. GT2006-90067.
[5] Land, C. C., Thole, K. A., and Joe, C., 2008, "Considerations of a Double-Wall Cooling Design to Reduce Sand Blockage," ASME Paper No. GT2008-50160.
[6] Poulton, P., and Cole, B.N., 1981, "An Experimental and Numerical Investigation of Louvred Inertia Air Filter Performance," Proceedings of the Conference on Gas Born Particles, Institution of Mechanical Engineers, Oxford, UK, June, pp. 161–170.

[7] Smith, J. L., Jr., and Goglia, M. J., 1956, "Mechanism of Separation in Louver-Type Dust Separator," ASME Trans. **78**(2), pp. 389–399.
[8] Gee, D. E., and Cole, B. N., 1969, "A Study of the Performance of Inertia Air Filters," Proceedings of the Institute of Mechanical Engineers—Symposium on Fluid Mechanics and Measurements in Two-Phase Systems, University of Leeds, Leeds, UK, pp. 167–176.
[9] Zverev, N. I., 1946, "Shutter-Type Dust Collector of Small Dimensions," Eng. Dig., **7**(11), pp. 353–355.
[10] Schneider, O., Dohmen, H. J., and Reichert, A. W., 2002, "Experimental Analysis of Dust Separation in the Internal Cooling Air System of Gas Turbines," ASME Paper No. GT2002-30240.
[11] Schneider, O., Dohmen, H. J., Benra, F.-K., and Brillert, D., 2003, "Investigations of Dust Separation in the Internal Cooling Air System of Gas Turbines," ASME Paper No. GT2003-38293.
[12] Schneider, O., Dohmen, H. J., Benra, F.-K., and Brillert, D., 2004, "Dust Separation in a Gas Turbine Pre-Swirl Cooling Air System, a Parameter Variation," ASME Paper No. GT2004-53048.
[13] Schneider, O., Benra, F.-K., Dohmen, H. J., and Jarzombek, K., 2005, "A Contribution to the Abrassive Effect of Particles in a Gas Turbine Pre-Swirl Cooling Air System," ASME Paper No. GT2005-68188.
[14] Villora, N. G., Dullenkopf, K., and Bauer, H. J., "Separation of Particles in the Secondary Air System of Gas Turbines," ASME Paper No. GT2011-45080.
[15] Syred, C., Griffiths, A., and Syred, N., 2004, "Gas Turbine Combustor With Integrated Ash Removal for Fine Particulates," ASME Paper No. GT2004-53270.
[16] Musgrove, G. O., Barringer, M. D., Thole, K. A., Grover, E., and Barker, J., 2009, "Computational Design of a Louver Particle Separator for Gas Turbine Engines," ASME Paper No. GT2009-60199.
[17] Powder Technology, Inc., 2009, Burnsville, MN.
[18] ANSYS, Inc., 2009, FLUENT Version 6.3.26, ANSYS Inc., NH.
[19] Moffat, R. J., 1988, "Describing the Uncertainties in Experimental Results," Exp. Thermal Fluid Sci., **1**, pp. 3–17.
[20] Schetz, J., and Fuhs, A., 1996, *Handbook of Fluid Dynamics and Fluid Machinery*, Vol. 1, John Wiley & Sons, Inc., New York, Chap. 14.